THE JOURNAL OF PHYSICAL CHEMISTRY B

Article

Cite This: J. Phys. Chem. B 2018, 122, 10653−10658

pubs.acs.org/JPCB

Correlating Conformational Dynamics with the Von Willebrand Factor Reductase Activity of Factor H Using Single Molecule Force Measurements

Sithara S. Wijeratne,[†,∥] Leticia Nolasco,[‡] Jingqiang Li,[†] Kevin Jiang,[§] Joel L. Moake,[‡] and Ching-Hwa Kiang*[,†,‡]

[†]Department of Physics and Astronomy, [‡]Department of Bioengineering, and [§]Department of Economics, Rice University, Houston, Texas 77005-1892, United States

ABSTRACT: Activation of proteins often involves conformational transitions, and these switches are often difficult to characterize in multidomain proteins. Full-length factor H (FH), consisting of 20 small consensus repeat domains (150 kD), is a complement control protein that regulates the activity of the alternative complement pathway. Different preparations of FH can also reduce the disulfide bonds linking large Von Willebrand factor (VWF) multimers into smaller, less adhesive forms. In contrast, commercially available purified FH (pFH) has little or no VWF reductase activity unless the pFH is chemically modified by either ethylenediaminetetraacetic acid (EDTA) or urea. We used atomic force microscopy single molecule force measurements to investigate different forms of FH, including recombinant FH and pFH, in the presence or absence of EDTA and urea, and to correlate the conformational changes to its activities. We found that the FH conformation depends on the method used for sample preparation, which affects the VWF reductase activity of FH.

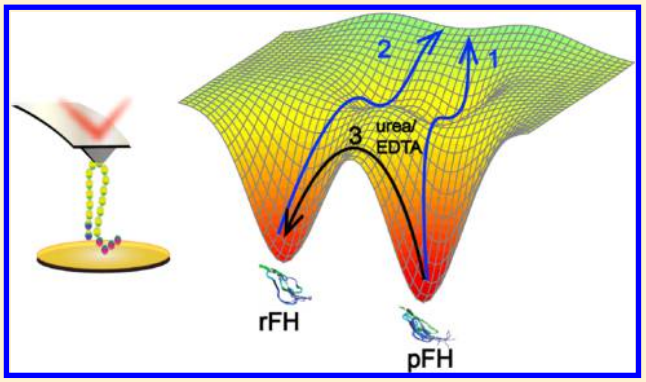

INTRODUCTION

Von Willebrand factor (VWF) is an essential protein in the hemostatic system that mediates the adhesion of platelets to the damaged vascular site by binding to platelet membrane glycoproteins.[1−3] The multimeric state of VWF is important for its platelet binding properties, with larger size VWF multimers being more hemostatically active.[4] Ultralarge VWF multimers secreted by, and anchored to, endothelial cells are the most hyperadhesive to platelets and, in cell-anchored form, are cleaved by the metalloprotease, ADAMTS-13. Cleaved, soluble VWF multimers in a wide range of sizes are generated.[5,6] Large soluble VWF multimers are also hyperadhesive to platelets under flowing conditions but cannot be cleaved by ADAMTS-13. We demonstrated[7] that a plasma complement regulatory protein, factor H (FH), reduces large soluble VWF forms into smaller, less adhesive multimeric sizes. This reductase function of FH may suppress platelet aggregation mediated by large soluble VWF multimers under arterial levels of fluid shear stress.[6] In this article, we describe conformational properties of FH necessary for its reductase activity on large soluble VWF multimers.

Members of the FH family of proteins are present in the plasma in several sizes ranging from 24 to 150 kD.[7−10] Full-length human FH negatively regulates the alternative complement pathway that is an important part of innate immune defense.[11] Full-length human FH is a 150 kD, single-chain plasma glycoprotein composed of 20 covalently linked, homologous subunits known as short consensus repeats (SCRs) or sushi domains because of their structural appearance. Each subunit sushi domain contains about 60 amino acids and 4 free cysteines (or 2 disulfide bonds) and is linked to neighboring subunits by nonsulfhydryl short linking elements.[12−15]

Both full-length FH purified from human plasma or prepared as human recombinant FH (rFH) had molecular weight values of 150 kD and were capable of reducing large soluble VWF multimers into smaller forms.[7] This is a nonproteolytic reduction that is unrelated to the VWF-cleaving enzyme, ADAMTS13.[5,16,17] It is not yet known if a deficiency or defect of FH-associated VWF reductase activity in human plasma leads to a shift toward large soluble VWF multimers in circulation, causing a propensity for the excessive shear-induced platelet aggregation (and thrombosis) observed in vitro.[18]

In contrast to human full-length FH of 150 kD purified in our own laboratory, commercially available purified FH (pFH) has a different migration speed in the polyacrylamide gel, showing a band at 130 kD, which is the apparent molecular mass (M_r) that depends on the molecule's conformational state. Also in contrast to rFH, pFH does not have the capacity

Received: June 27, 2018
Revised: September 6, 2018
Published: October 10, 2018

DOI: 10.1021/acs.jpcb.8b06153
J. Phys. Chem. B 2018, 122, 10653−10658

to reduce large soluble VWF multimers into smaller sizes. However, treatment of pFH with chemicals such as urea and ethylenediaminetetraacetic acid (EDTA) restored the VWF-reducing activity of pFH. During the exposure to urea or EDTA, the chemically treated pFH is shifted to an apparent M_r of 150 kD. We hypothesize that this chemical treatment restores the VWF reductase activity of pFH by shifting its conformational state. This is an effect analogous to the shear-induced activation of VWF.[19−23]

We proceeded to study the characteristics of full-length human FH, using rFH and pFH with and without chemical treatment (urea or EDTA), using single molecule manipulation with atomic force microscopy (AFM). It has been shown that AFM studies can reveal the dynamics of VWF conformational changes.[20,24,25] Single rFH and pFH molecules were stretched by AFM and the force peaks indicated the unfolding of the sushi domain of FH, similar to other protein unfolding studies.[26−32]

We have also evaluated the effect of solvent (tri-*n*-butyl phosphate)−detergent (Triton X-100) treatment on rFH structure and reductase activity for VWF multimers. This type of solvent−detergent (SD) treatment of plasma-derived components has been used in transfusion therapy to inactivate viruses with lipid envelopes [hepatitis B virus (HBV) and hepatitis C virus (HCV) and human immunodeficiency virus (HIV)-(1)].

EXPERIMENTAL METHODS

The production of rFH using baculovirus[33] or yeast[34] systems has been reported. We used human embryonic kidney (HEK) 293 cells [American Type Culture Collection (ATCC), Mananssas, VA] to generate FH. Full-length human FH cDNA was generated by polymerase chain reaction with 5′ primer (GGACTTTCCAAAATGTCGT) and 3′ primer (ATCCTCGAGCTCTTTTTGCACAAGT), using human FH cDNA (Origene Technologies, Inc., Rockville, MD) as a template. After confirming the sequence, the amplified DNA fragment was digested with Not I (5′) and Xho I (3′) and ligated to pSecTag2B his tag vector (Invitrogen, Grand Island, NY). The plasmid containing full-length FH cDNA was transfected into HEK 293 cells using Lipofectamine 2000 (Invitrogen, Carlsbad, CA), which were maintained in Dulbecco's modified Eagle medium containing 10% fetal bovine serum (Atlanta Biologicals, Lawrenceville, GA), 1 mM sodium pyruvate 1% minimal essential medium-nonessential amino acids, and the selection agent, Hygromycin B (250 μg/mL) (Enzo, Farmingdale, NY). rFH released from the HEK 293 cells into the culture media was purified using his-select Ni^{2+}-charged affinity gel (Sigma Chemicals, St. Louis, MO) that binds to histidine-tagged rFH. Briefly, serum-free conditioned cell culture medium was purified using 6× his-select resin. His-tagged proteins were then eluted using 250 mM imidazole. pFH is commercially available (Comptech, Tyler, Texas and Quidel, San Diego, CA). The pFH has been chemically treated to maintain stability for commercial purposes.

FH molecules were equilibrated at 37 °C prior to being deposited onto a fresh gold surface at room temperature. All experiments were done in a fluid environment in phosphate-buffered saline (PBS) buffer. Segments of the FH molecules attached to the gold substrate were pulled using the AFM tip (MLCT, Bruker, Camarillo, CA) by nonspecific adsorption on one end and to the substrate on the other end with pulling velocities ranging from 500 nm/s to 2 μm/s.

To test for FH-related VWF-reducing activity, soluble VWF multimers (containing ultralarge VWF forms) released from human umbilical vein endothelial cells (HUVECs) were mixed with the various types of FH (pFH, rFH, pFH + urea, pFH + EDTA; 50/50 vol/vol) and incubated at room temperature for 15 min. The mixture was denatured using 8 M urea-Tris-1% sodium dodecyl sulfate (SDS), electrophoresed into SDS-1% agarose gel, and electrotransferred onto an immobilon poly(vinylidene difluoride) (PVDF) membrane (Millipore Corporation, Billerica, MA). The transferred protein was detected using rabbit anti-human VWF (Ramco Laboratories, Houston, TX) and a secondary goat anti-rabbit antibody linked to horse radish peroxidase (HRP)[7] (Thermo Scientific, Rockford, Il) and then chemiluminescent reagent (Thermo Scientific). Results were recorded using a BioRad Gel Doc XR imager (BioRad Laboratories, Hercules, CA).

The rFH and pFH samples were electrophoresed into a 7% nonreduced SDS-polyacrylamide gel, electrotransferred onto a PVDF membrane, and detected using goat anti-human FH (Complement Technologies, Tyler, TX) and a secondary rabbit anti-goat antibody linked to HRP (Thermo Scientific, Waltham, MA).

Ellman's reagent (5,5-dithiobis-2 nitrobenzoic acid) (Sigma, Chemicals, St. Louis, MO) was used to quantify thiol groups in the samples of rFH (0.905−1.420 μg/mL) and pFH (100 μg/mL) by the absorption measurement. Free thiols were calculated from a standard curve constructed using known cysteine concentrations in a range of 0.125−1.5 mM. Iodoacetic acid (1 mM) was used to inhibit free thiols and blocked the disulfide bonds to prevent reformation (n = 4).

SD treatment of rFH consisted of treating his-tagged rFH with 1% solvent (tri-*n*-butyl phosphate) and 1% detergent (Triton-X) for 4 h at 30 °C to stabilize the VWF-reducing activity and to eliminate HIV, HBV, and HCV. Added reagents were removed by extraction with 5% soybean oil, high-speed centrifugation, chromatography on Prep C18 resin, dialyzed, and concentrated.[7] The amount of rFH before and after SD treatment was quantified using an enzyme-linked immunosorbent assay.

RESULTS

We pulled single FH molecules using AFM and acquired their force−extension curves as shown in Figure 1. Typical force−extension curves of pFH and rFH, using a pulling speed of 0.5 μm/s, showed characteristic saw-tooth patterns resulting from protein domain unfolding.[20,24] The unfolding peaks in the force curves were fitted with the worm-like chain (WLC) model[37−39] as follows:

$$F(x) = \frac{k_B T}{L_p}\left[\frac{1}{4(1 - x/L_c)^2} + \frac{x}{L_c} - \frac{1}{4}\right] \quad (1)$$

where x is the distance; F is the force; k_B is the Boltzmann constant; T is the temperature; and L_p and L_c are the persistence length and contour length, respectively.

Histograms of the force peaks were compiled, and distributions were fitted to a Gaussian curve. The peaks of these Gaussian curves represent the most probable values. The force of the last peak in each force−extension curve is not included in the histogram because it corresponds to the detachment force from the substrate or AFM tip. The

DOI: 10.1021/acs.jpcb.8b06153
J. Phys. Chem. B 2018, 122, 10653−10658

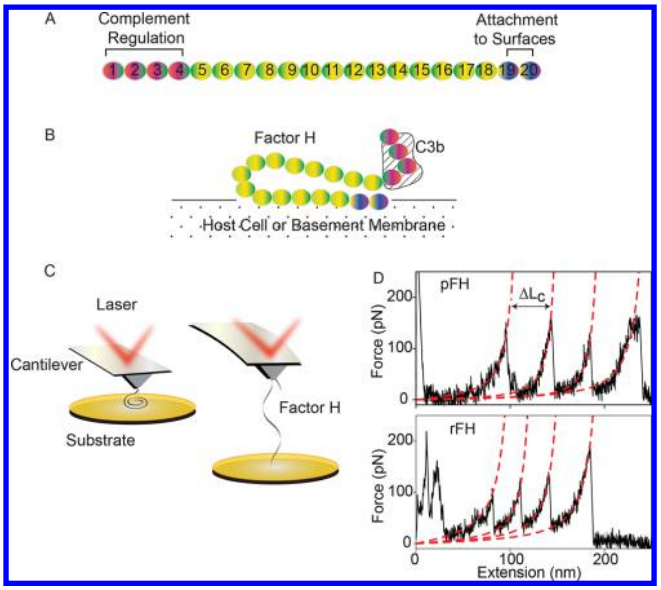

Figure 1. AFM experimental setup of FH. (A) Full-length FH is composed of 20 SCR sushi domains. (B) FH binds to C3b (functional C3) and promotes C3b proteolytic degradation by the proteolytic enzyme, factor I. (C) Experimental setup for AFM experiments. (D) Force–extension curves of pFH and rFH. Dashed lines are WLC model fit of the unfolding force curves.[35] ΔL_c is the change in contour length of the stretched protein and is a measure of the length of an unfolded domain.[36]

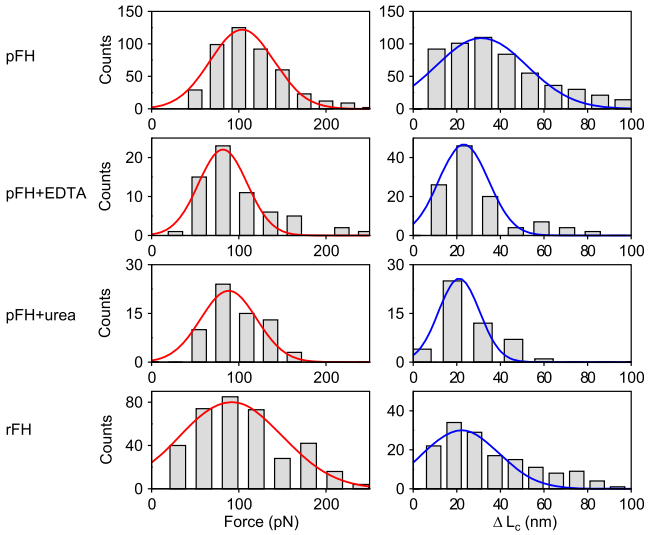

Figure 2. Histograms of unfolding of different forms of FH. The unfolding force peak values in the force vs distance curves (Figure 1D) were compiled into histograms, which were then fitted to a Gaussian distribution to determine the most probable peak force value (solid red lines). At 0.5 μm/s pulling speed, the most probable peak values of pFH (no VWF reductase activity) = 104 pN (n = 3); pFH + EDTA (VWF reductase activity) = 82 pN (n = 3); pFH + urea (VWF reductase activity) = 89 pN (n = 4); and rFH = 91 pN (n = 4). n is the number of sample batches used to obtain the distribution. Histograms of the changes in contour length, ΔL_c, of different FH forms were also fitted to Gaussian distribution, which have a major peak at 32 nm for pFH, 23 nm for pFH + EDTA, 21 nm for pFH + urea, and 22 nm for rFH. The force and ΔL_c values are in the range of protein unfolding.[38,42,44]

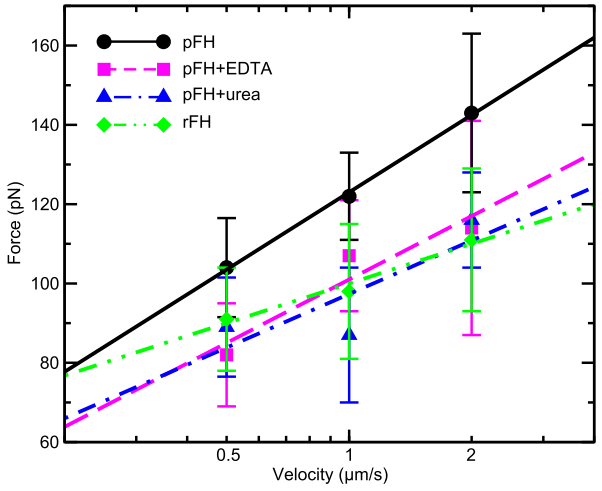

Figure 3. Velocity-dependent unfolding forces of pFH and rFH. The most probable unfolding forces of pFH (n = 7), rFH (n = 13), pFH + EDTA (n = 8), and pFH + urea (n = 9) for pulling velocities from 0.5 to 2 μm/s. The peak unfolding forces of different forms of FH with VWF reductase activity (rFH, pFH + urea, pFH + EDTA) are consistently lower than those without VWF reductase activity (pFH).

distributions of unfolding forces and changes in contour length are shown in Figure 2. The change in contour length determined using ΔL_c corresponds to the added length from domain unfolding and is proportional to the number of amino acids per domain. The ΔL_c ranges from 21 to 32 nm, which is consistent with the unfolding of a single 60-residue sushi domain of FH using 0.36 nm as the length of a residue.[5,40,41] The unfolding force is also consistent with those of protein domain unfolding.[38,42−44] The velocity-dependent unfolding forces[43] of different forms of FH, shown in Figure 3, demonstrate that the peak unfolding forces of FH with VWF reductase activity (rFH; pFH + urea; pFH + EDTA) are consistently lower than that of untreated pFH, which has no VWF reductase activity. The difference in unfolding peak forces suggests different conformations, which results in different transition states.[20,24,30]

Free thiols were quantified using Ellman's reagent (5,5′-dithio-bis-2-nitrobenzoic acid). pFH contains fewer free thiols compared to rFH. rFH (0.905−1.420 μg/mL) at 1/100 of the concentration of pFH (100 μg/mL) has about 5-fold more exposed free thiols than pFH. pFH treated with either 1 M urea or 10 mM EDTA showed 25−40% increase in free thiols. However, the absolute number of free thiols remained small.

Figure 4 demonstrates that pFH migrates into SDS-polyacrylamide gels with a higher mobility (apparent M_r = 130 kD) than rFH (apparent M_r = 150 kD). pFH in PBS (310 ng/well final concentration) had an apparent M_r of 130 kD in an unreduced SDS-7% polyacrylamide gel. After incubation overnight at 4 °C with either 10 mM EDTA or 1 M urea (that had been adjusted to pH 7.6), the apparent M_r values of both chemically treated pFH samples were shifted to a slower migration with an apparent M_r of 150 kD. When untreated pFH (31 μg/mL; final concentration) was mixed 1:1 with soluble HUVEC-secreted VWF multimers (2−3% of normal human plasma VWF antigen), little or no VWF reductase activity was observed. In contrast, when VWF multimers were mixed 1:1 with either urea-treated pFH or EDTA-treated pFH, the chemically treated pFH showed VWF-reducing activity. Incubation with either urea or EDTA alters the conformation of pFH, slows the migration of pFH, and imbues the treated pFH with VWF reductase activity. This alteration in the

DOI: 10.1021/acs.jpcb.8b06153
J. Phys. Chem. B 2018, 122, 10653−10658

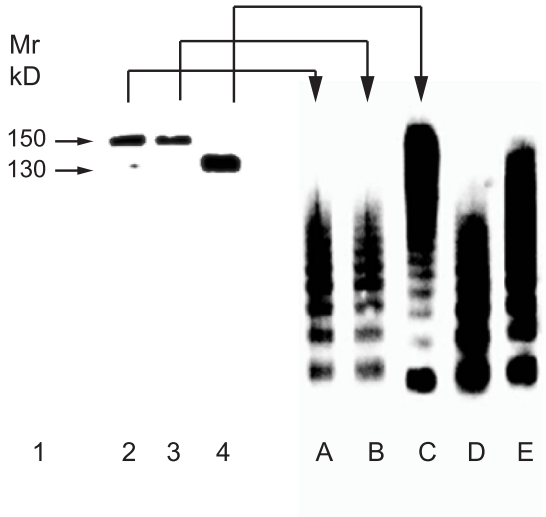

Figure 4. VWF multimer reductase activity of pFH was acquired by exposure to either EDTA or urea. Lane 1, apparent M_r values; lane 2, pFH + urea; lane 3, pFH + EDTA; lane 4, pFH. Lane D, normal human plasma VWF multimers. Lane E, HUVEC-secreted VWF multimers (including ultralarge, a more slowly migrating, VWF forms). Lane C, sample from lane 4 + sample from lane E. Lane A, sample from lane 2 + sample from lane E. Lane B, sample from lane 3 + sample from lane E. In lanes 2−4, the unreduced samples were electrophoresed into an SDS-7% polyacrylamide gel, the protein was transferred onto a PVDF membrane, analyzed using rabbit anti-human FH plus goat anti-rabbit-HRP, and detected using a chemiluminescent substrate. In lanes A−E, the mixed samples were electrophoresed into an SDS-1% agarose gel, transferred onto a PVDF membrane, analyzed by rabbit anti-human VWF + goat anti-rabbit-HRP, and detected by a chemiluminescent substrate (n = 6).

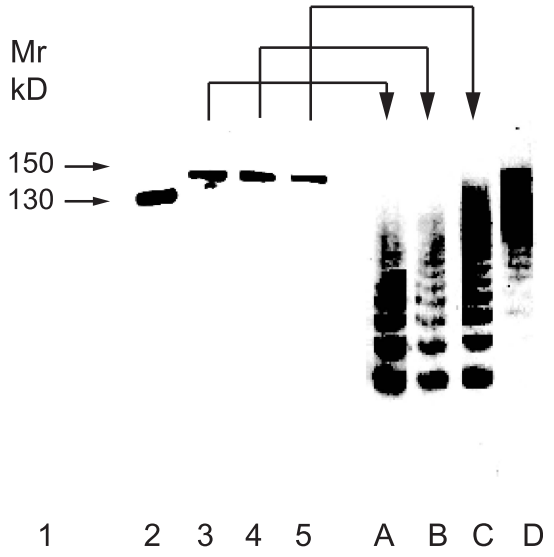

Figure 5. SD treatment of human rFH. Solvent (tri-*n*-butyl phosphate) and detergent (Triton X-100) (SD) treatment (to inactivate envelope viruses) of rFH does not prevent rFH-mediated reduction of VWF multimers. Lanes 1−5, Western blot of unreduced SDS 4−12% polyacrylamide gel. Lane 1, the relative mobility of molecular weight markers (apparent M_r). Lane 2, pFH, apparent M_r 130 kD. Lanes 3−5, rFH: lane 3, purified, SD-treated; lane 4, purified, non-SD-treated; lane 5, nonpurified, non-SD-treated. Lanes A−D, Western blot of unreduced SDS-1% agarose gel. Lane D, serum-free conditioned media from cultured HUVECs containing VWF multimers (including ultralarge VWF forms) were used as the substrate to test for FH-mediated reductase activity. The mixed samples are from lane 3 + lane D in lane A; lane 4 + lane D in lane B; and lane 5 + lane D in lane C. Concentrations in lanes 2−5 are the same as in the legend of Figure 4. In lanes 1−5, samples under nonreducing conditions were electrophoresed into SDS 4−12% polyacrylamide gel electrophoresis, electrotransferred onto a PVDF membrane, analyzed by rabbit anti-human FH + goat anti-rabbit-HRP, and detected by chemiluminescence. In lanes A−D, samples were electrophoresed into an SDS-1% agarose gel, electrotransferred onto a PVDF membrane and analyzed by rabbit anti-human VWF + goat anti-rabbit-HRP, and detected using chemiluminescence (n = 3).

conformation of pFH occurs in association with its shift to slower mobility (apparent M_r = 150 kD, which is similar to that of rFH).

After treatment of rFH with solvent (tri-*n*-butyl phosphate) and detergent (Triton X-100) for 4 h at 30 °C, the VWF reductase activity of the treated rFH was not changed (Figure 5). All of these rFH proteins, SD-treated or not, had apparent M_r values of 150 kD and VWF reductase activity when mixed 1:1 vol/vol with HUVEC-released VWF multimers (that include ultralarge VWF forms; 3% of the VWF antigen level in normal human plasma). The nonpurified rFH in lane 5 had a lower VWF reductase activity (and contained a lower amount of rFH) than the two purified, concentrated rFH samples (containing a greater quantity of rFH).

DISCUSSION

Our results demonstrate that pFH has a smaller apparent molecular mass (130 kD), fewer exposed free thiols, and little or no reductase activity for soluble VWF multimers. Treatment with urea or EDTA converts the conformation of pFH molecules into a slower gel migration position at apparent M_r = 150 kD (with a slight increase in exposed free thiols) and the capacity to reduce soluble VWF multimers. These are characteristics that are similar to those of rFH (treated or untreated with SD). Our data suggest that the conformation of full-length FH determines the capacity of FH to reduce large soluble VWF multimers.

This interpretation was supported by the results from single molecule force studies. We compared data from the AFM forced unfolding of different forms of FH. The change in contour length of pFH without VWF reductase activity was greater than that of other forms of FH (rFH, pFH + urea, and pFH + EDTA) that have VWF reductase activity. These results suggest that the domains of untreated pFH are in a more compact state than the domains of the other forms of FH with VWF reductase activity. A less compact conformation, essential for VWF reductase activity, can be induced in pFH by exposing the pFH to urea or EDTA. The other forms of FH evaluated in this study that either already have (rFH) or can be chemically altered (pFH + urea or pFH + EDTA) to obtain VWF reductase activity are in a less compact state and are less resistant to forced unfolding (Figure 6).[20,45−50]

CONCLUSIONS

Our single molecule AFM experiments indicate that FH prepared by different methods has different conformations that determine its capacity to reduce VWF multimers. Furthermore, the VWF reductase activity of rFH is not affected by SD treatment that is used to inactivate lipid envelope viruses. This latter finding may prove useful in the preparation of rFH or other full-length forms of FH with VWF reductase activity for therapeutic use.

DOI: 10.1021/acs.jpcb.8b06153
J. Phys. Chem. B 2018, 122, 10653−10658

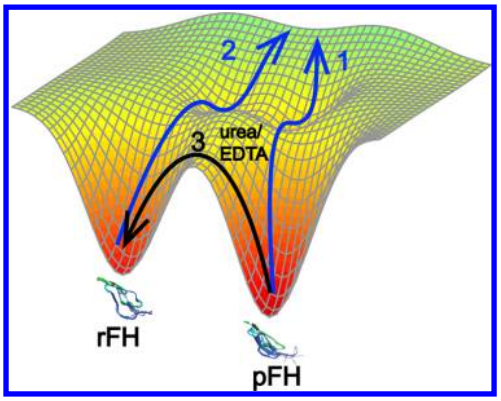

Figure 6. Illustration of free energy landscape of different forms of FH. pFH has no VWF reductase activity and is in a more compact conformation. Stretching of pFH molecules results in domain unfolding (pathway 1), whereas the domain unfolding of rFH follows a different pathway (pathway 2). The barrier height of pathways 1 and 2 corresponds to the different unfolding peak forces. Treatment of urea or EDTA switches pFH to a less compact form of FH (pathway 3) that is similar to rFH in conformation and VWF reductase activity.

AUTHOR INFORMATION

Corresponding Author

*E-mail: chkiang@rice.edu. Phone: 713-348-4130.

ORCID

Ching-Hwa Kiang: 0000-0001-7162-9680

Present Address

[‖]Department of Genetics, Harvard Medical School and Department of Molecular Biology, Massachusetts General Hospital, Boston, Massachusetts, USA.

Notes

The authors declare no competing financial interest.

ACKNOWLEDGMENTS

This work was supported by the National Science Foundation (0907676), the Welch Foundation (C-1632), the Hamill Foundation, the Mary Rodes Gibson Foundation, and the Hinkson Memorial Fund. We appreciate the FH plasmid kindly provided by Dr. Shuju Feng and Dr. Vahid Afshar-khargan.

REFERENCES

(1) Ruggeri, Z. M. Von Willebrand Factor. *Curr. Opin. Hematol.* **2003**, *10*, 142−149.

(2) Sadler, J. E. Biochemistry and Genetics of Von Willebrand Factor. *Annu. Rev. Biochem.* **1998**, *67*, 395−424.

(3) Zhang, X.; Zhang, W.; Dragovich, M.; Deng, W.; Li, R. Biophysical Characterization of Mechanosensors within the Plasma Protein Von Willebrand Factor and its Receptor Platelet Glycoprotein IB-IX. *Biophys. J.* **2016**, *110*, 637a.

(4) Crawley, J. T. B.; de Groot, R.; Xiang, Y.; Luken, B. M.; Lane, D. A. Unraveling the Scissile Bond: How ADAMTS13 Recognizes and Cleaves Von Willebrand Factor. *Blood* **2011**, *118*, 3212−3221.

(5) Zhang, X.; Halvorsen, K.; Zhang, C.-Z.; Wong, W. P.; Springer, T. A. Mechanoenzymatic Cleavage of the Ultralarge Vascular Protein Von Willebrand Factor. *Science* **2009**, *324*, 1330−1334.

(6) Turner, N.; Nolasco, L.; Moake, J. Generation and Breakdown of Soluble Ultralarge Von Willebrand Factor Multimers. *Semin. Thromb. Hemost.* **2012**, *38*, 38−46.

(7) Nolasco, L.; Nolasco, J.; Feng, S.; Afshar-Kharghan, V.; Moake, J. Human Complement Factor H is a Reductase for Large Soluble Von Willebrand Factor Multimers-Brief Report. *Arterioscler. Thromb. Vasc. Biol.* **2013**, *33*, 2524−2528.

(8) Ripoche, J.; Day, A. J.; Harris, T. J. R.; Sim, R. B. The Complete Amino Acid Sequence of Human Complement Factor H. *Biochem. J.* **1988**, *249*, 593−602.

(9) Turner, N. A.; Moake, J. Assembly and Activation of Alternative Complement Components on Endothelial Cell-Anchored Ultra-Large Von Willebrand Factor Links Complement and Hemostasis-Thrombosis. *PloS One* **2013**, *8*, No. e59372.

(10) Turner, N. A.; Moake, J. L. Regulatory Components of the Alternative Complement Pathway in Endothelial Cell Cytoplasm, Factor H and Factor I, are Not Packaged in Weibel-Palade Bodies. *PloS One* **2015**, *10*, No. e0140740.

(11) Pangburn, M. K. Host Recognition and Target Differentiation by Factor H, a Regulator of the Alternative Pathway of Complement. *Immunopharmacology* **2000**, *49*, 149−157.

(12) Józsi, M.; Zipfel, P. F. Factor H Family Proteins and Human Diseases. *Trends Immunol.* **2008**, *29*, 380−387.

(13) Gordon, D. L.; Kaufman, R. M.; Blackmore, T. K.; Kwong, J.; Lublin, D. M. Identification of Complement Regulatory Domains in Human Factor-H. *J. Immunol.* **1995**, *155*, 348−356.

(14) Zipfel, P. F. Complement Factor H: Physiology and Pathophysiology. *Semin. Thromb. Hemost.* **2001**, *27*, 191−200.

(15) Morgan, H. P.; Mertens, H. D. T.; Guariento, M.; Schmidt, C. Q.; Soares, D. C.; Svergun, D. I.; Herbert, A. P.; Barlow, P. N.; Hannan, J. P. Structural Analysis of the C-Terminal Region (Modules 18-20) of Complement Regulator Factor H (FH). *PloS One* **2012**, *7*, No. e32187.

(16) Feng, S.; Liang, X.; Cruz, M. A.; Vu, H.; Zhou, Z.; Pemmaraju, N.; Dong, J.-F.; Kroll, M. H.; Afshar-Kharghan, V. The Interaction between Factor H and Von Willebrand Factor. *PloS One* **2013**, *8*, No. e73715.

(17) Interlandi, G.; Ling, M.; Tu, A. Y.; Chung, D. W.; Thomas, W. E. Structural Basis of Type 2A Von Willebrand Disease Investigated by Molecular Dynamics Simulations and Experiments. *PloS One* **2012**, *7*, No. e45207.

(18) Wick, T. M.; Moake, J. L.; Udden, M. M.; Eskin, S. G.; Sears, D. A.; McIntire, L. V. Unusually Large Von Willebrand Factor Multimers Increase Adhesion of Sickle Erythrocytes to Human Endothelial Cells under Controlled Flow. *J. Clin. Invest.* **1987**, *80*, 905−910.

(19) Huck, V.; Gorzelanny, C.; Schneider, M.; Schneider, S. The Various States of Von Willebrand Factor and Their Function in Physiology and Pathophysiology. *Thromb. Haemostasis* **2014**, *111*, 598−609.

(20) Wijeratne, S. S.; Botello, E.; Yeh, H.-C.; Zhou, Z.; Bergeron, A. L.; Frey, E. W.; Patel, J. M.; Nolasco, L.; Turner, N. A.; Moake, J. L.; Dong, J.-F.; Kiang, C.-H. Mechanical Activation of a Multimeric Adhesive Protein through Domain Conformational Change. *Phys. Rev. Lett.* **2013**, *110*, 108102.

(21) Baldauf, C.; Schneppenheim, R.; Stacklies, W.; Obser, T.; Pieconka, A.; Schneppenheim, S.; Budde, U.; Zhou, J.; Gräter, F. Shear-Induced Unfolding Activates Von Willebrand Factor A2 Domain for Proteolysis. *J. Thromb. Haemostasis* **2009**, *7*, 2096−2105.

(22) Alexander-Katz, A.; Schneider, M. F.; Schneider, S. W.; Wixforth, A.; Netz, R. R. Shear-Flow-Induced Unfolding of Polymeric Globules. *Phys. Rev. Lett.* **2006**, *97*, 138101.

(23) Vergauwe, R. M. A.; Uji-i, H.; De Ceunynck, K.; Vermant, J.; Vanhoorelbeke, K.; Hofkens, J. Shear-Stress-Induced Conformational Changes of Von Willebrand Factor in a Water-Glycerol Mixture Observed with Single Molecule Microscopy. *J. Phys. Chem. B* **2014**, *118*, 5660−5669.

(24) Wijeratne, S. S.; Li, J.; Yeh, H.-C.; Nolasco, L.; Zhou, Z.; Bergeron, A.; Frey, E. W.; Moake, J. L.; Dong, J.-F.; Kiang, C.-H. Single-Molecule Force Measurements of the Polymerizing Dimeric Subunit of Von Willebrand Factor. *Phys. Rev. E* **2016**, *93*, 012410.

(25) Müller, J. P.; Mielke, S.; Löf, A.; Obser, T.; Beer, C.; Bruetzel, L. K.; Pippig, D. A.; Vanderlinden, W.; Lipfert, J.; Schneppenheim, R.; Benoit, M. Force Sensing by the Vascular Protein Von Willebrand

DOI: 10.1021/acs.jpcb.8b06153
J. Phys. Chem. B 2018, 122, 10653−10658

Factor is Tuned by a Strong Intermonomer Interaction. *Proc. Natl. Acad. Sci. U.S.A.* **2016**, *113*, 1208−1213.
(26) Alsteens, D.; Martinez, N.; Jamin, M.; Jacob-Dubuisson, F. Sequential Unfolding of Beta Helical Protein by Single-Molecule Atomic Force Microscopy. *PloS One* **2013**, *8*, No. e73572.
(27) Carrion-Vazquez, M.; Oberhauser, A. F.; Fowler, S. B.; Marszalek, P. E.; Broedel, S. E.; Clarke, J.; Fernandez, J. M. Mechanical and Chemical Unfolding of a Single Protein: A Comparison. *Proc. Natl. Acad. Sci. U.S.A.* **1999**, *96*, 3694−3699.
(28) Marszalek, P. E.; Lu, H.; Li, H.; Carrion-Vazquez, M.; Oberhauser, A. F.; Schulten, K.; Fernandez, J. M. Mechanical Unfolding Intermediates in Titin Modules. *Nature* **1999**, *402*, 100−103.
(29) Kim, M.; Abdi, K.; Lee, G.; Rabbi, M.; Lee, W.; Yang, M.; Schofield, C. J.; Bennett, V.; Marszalek, P. E. Fast and Forceful Refolding of Stretched a-Helical Solenoid Proteins. *Biophys. J.* **2010**, *98*, 3086−3092.
(30) Serquera, D.; Lee, W.; Settanni, G.; Marszalek, P. E.; Paci, E.; Itzhaki, L. S. Mechanical Unfolding of an Ankyrin Repeat Protein. *Biophys. J.* **2010**, *98*, 1294−1301.
(31) Botello, E.; Harris, N. C.; Sargent, J.; Chen, W.-H.; Lin, K.-J.; Kiang, C.-H. Temperature and Chemical Denaturant Dependence of Forced Unfolding of Titin 127. *J. Phys. Chem. B* **2009**, *113*, 10845−10848.
(32) Hoffmann, T.; Tych, K. M.; Brockwell, D. J.; Dougan, L. Single-Molecule Force Spectroscopy Identifies a Small Cold Shock Protein as Being Mechanically Robust. *J. Phys. Chem. B* **2013**, *117*, 1819−1826.
(33) Sharma, A. K.; Pangburn, M. K. Biologically Active Recombinant Human Complement Factor H: Synthesis and Secretion by the Baculovirus System. *Gene* **1994**, *143*, 301−302.
(34) Schmidt, C. Q.; Slingsby, F. C.; Richards, A.; Barlow, P. N. Production of Biologically Active Complement Factor H in Therapeutically Useful Quantities. *Protein Expr. Purif.* **2011**, *76*, 254−263.
(35) Guo, C.-L.; Harris, N. C.; Wijeratne, S. S.; Frey, E. W.; Kiang, C.-H. Multiscale Mechanobiology: Mechanics at the Molecular, Cellular, and Tissue Levels. *Cell Biosci.* **2013**, *3*, 25.
(36) Chen, W.-H.; Wilson, J. D.; Wijeratne, S. S.; Southmayd, S. A.; Lin, K.-J.; Kiang, C.-H. Principles of Single-Molecule Manipulation and its Application in Biological Physics. *Int. J. Mod. Phys. B* **2012**, *26*, 1230006.
(37) Bustamante, C.; Marko, J.; Siggia, E.; Smith, S. Entropic Elasticity of Lambda-Phage DNA. *Science* **1994**, *265*, 1599−1600.
(38) Rief, M.; Gautel, M.; Oesterhelt, F.; Fernandez, J. M.; Gaub, H. E. Reversible Unfolding of Individual Titin Immunoglobulin Domains by AFM. *Science* **1997**, *276*, 1109−1112.
(39) Yao, M.; Chen, H.; Yan, J. Thermodynamics of Force-Dependent Folding and Unfolding of Small Protein and Nucleic Acid Structures. *Integr. Biol.* **2015**, *7*, 1154−1160.
(40) Oesterhelt, F.; Oesterhelt, D.; Pfeiffer, M.; Engel, A.; Gaub, H. E.; Muller, D. J. Unfolding Pathways of Individual Bacteriorhodopsins. *Science* **2000**, *288*, 143−146.
(41) Winardhi, R. S.; Tang, Q.; Chen, J.; Yao, M.; Yan, J. Probing Small Molecule Binding to Unfolded Polyprotein Based on Its Elasticity and Refolding. *Biophys. J.* **2016**, *111*, 2349−2357.
(42) Fernandez, J. M.; Oberhauser, A. F.; Marszalek, P. E.; Erickson, H. P. The Molecular Elasticity of the Extracellular Matrix Protein Tenascin. *Nature* **1998**, *393*, 181−185.
(43) Harris, N. C.; Kiang, C.-H. Velocity Convergence of Free Energy Surfaces from Single-Molecule Measurements Using Jarzynski's Equality. *Phys. Rev. E: Stat., Nonlinear, Soft Matter Phys.* **2009**, *79*, 041912.
(44) Rief, M.; Pascual, J.; Saraste, M.; Gaub, H. E. Single Molecule Force Spectroscopy of Spectrin Repeats: Low Unfolding Forces in Helix Bundles. *J. Mol. Biol.* **1999**, *286*, 553−561.
(45) Frey, E. W.; Li, J.; Wijeratne, S. S.; Kiang, C.-H. Reconstructing Multiple Free Energy Pathways of DNA Stretching from Single Molecule Experiments. *J. Phys. Chem. B* **2015**, *119*, 5132−5135.
(46) Harris, N. C.; Song, Y.; Kiang, C.-H. Experimental Free Energy Surface Reconstruction from Single-Molecule Force Spectroscopy Using Jarzynski's Equality. *Phys. Rev. Lett.* **2007**, *99*, 068101.
(47) Cheung, M. S. Where Soft Matter Meets Living Matter - Protein Structure, Stability, and Folding in the Cell. *Curr. Opin. Struct. Biol.* **2013**, *23*, 212−217.
(48) Homouz, D.; Stagg, L.; Wittung-Stafshede, P.; Cheung, M. S. Macromolecular Crowding Modulates Folding Mechanism of Alpha/Beta Protein Apoflavodoxin. *Biophys. J.* **2009**, *96*, 671−680.
(49) Onuchic, J. N.; Luthey-Schulten, Z.; Wolynes, P. G. Theory of Protein Folding: The Energy Landscape Perspective. *Annu. Rev. Phys. Chem.* **1997**, *48*, 545−600.
(50) Schug, A.; Gambin, Y.; Deniz, A.; Onuchic, J. The Rop-Dimer: A Folded Protein Living between Two Alternate Structures. *Biophys. J.* **2009**, *96*, 568a.

DOI: 10.1021/acs.jpcb.8b06153
J. Phys. Chem. B 2018, 122, 10653−10658